

Jet tomography

Ivan Vitev†

† Iowa State University, Department of Physics and Astronomy,
12 Physics Building A330, Ames, IA 50011, USA

E-mail: ivitev@iastate.edu

Abstract. I summarize the recent advances in jet tomographic studies of cold and hot nuclear matter based on perturbative QCD calculations of medium-induced gluon bremsstrahlung. Quantitative applications to ultrarelativistic heavy ion reactions at RHIC indicate the creation of a deconfined state of QCD with initial energy density on the order of 100 times cold nuclear matter density.

Submitted to: *J. Phys. G: Nucl. Phys.*

1. Introduction

Tomography is the study of the properties of matter through the attenuation pattern of a calibrated flux of fast particles that lose energy via multiple elastic and inelastic scatterings. For ultrarelativistic heavy ion reactions this technique was first discussed for vector mesons but has only recently been generalized to hard partonic processes which dominate the experimentally accessible moderate- and high- p_T region of hadron production [1]. Jet tomography extracts the nuclear matter density from the modification to the differential hadron multiplicities $R_{AB}(b) = \left(\frac{dN_{AB}^h(b)}{dyd^2p_T} \right) / \left(\frac{T_{AB}(b)d\sigma_{pp}^h}{dyd^2p_T} \right)$. The overlap function $T_{AB}(b)$ reflects the reaction geometry and the elementary nucleon-nucleon cross sections are calculable to leading and next-to-leading order [2] based on the successful perturbative QCD factorization approach [3]. The potentially dramatic observable effects of jet quenching [4], $R_{AB} \sim \exp(-\int_0^L dz' \sigma_{\text{abs}}(z')\rho(z'))$, in $A+A$ versus $p+p$ collisions even for dynamically expanding systems come from the nuclear size enhancement $\propto r_0 A^{1/3}$ and the large initial energy and parton number densities of the quark-gluon plasma (QGP) created in the interaction region. In addition to the suppression of the single inclusive spectra [5] and the disappearance of the back-to-back di-hadron correlations [6] in central and semi-central $Au + Au$ reactions, parton energy loss plays a major role in the generation of the high- p_T azimuthal asymmetry [7] and the enhancement of the moderate- p_T baryon to meson ratios [8]. The final state origin of many of these effects is now confirmed via the control $d + Au$ measurement and its comparison to theoretical predictions [9, 10].

The first calculations of the Landau-Pomeranchuk-Migdal (LPM) destructive interference effect in QCD [11] already indicated that medium induced non-Abelian bremsstrahlung dominates over the elastic energy loss. The current techniques for

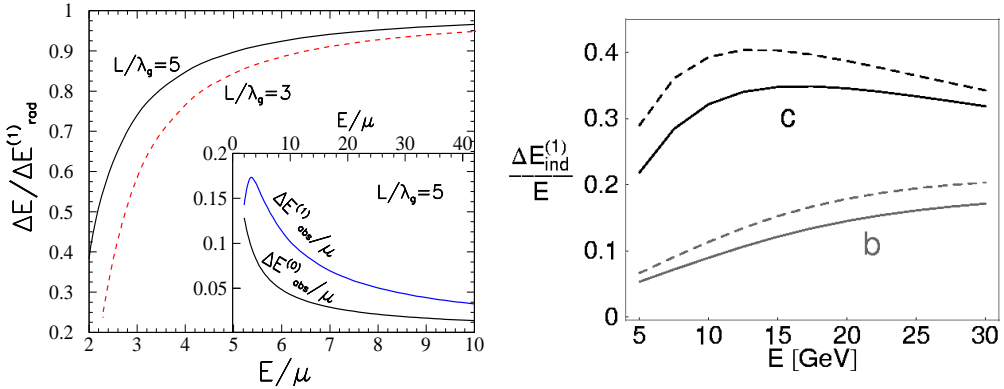


Figure 1. Left panel from [17]: reduction of the medium induced radiative energy loss via gluon absorption as a function of E/μ . Right panel from [19]: jet energy dependence of the mean fractional energy loss $\Delta E/E$. The sensitivity on the plasmon mass ω_{pl} and the heavy quark mass M_q is illustrated.

the computation of the gluon radiative spectrum $\frac{\omega dN^g}{d\omega}$ and the mean energy loss ΔE have been reviewed in [12] and include a path integral approach [13], an effective 2D Schrödinger equation [14], exact Reaction Operator formalism [15] and a twist expansion series [16]. For static non-Abelian media the mean energy loss depends quadratically on the nuclear size, $\Delta E = -\frac{C_R \pi \alpha_s}{4} \frac{\mu^2}{\lambda_g} L^2 \ln \frac{2E}{\mu^2 L} + \dots$, and measures the gluon transport coefficient $\hat{q} = \frac{\mu^2}{\lambda_g}$. In dynamically expanding plasmas the radiative spectrum and the mean energy loss can be related to the soft gluon rapidity density, $\Delta E = -\frac{9C_R \pi \alpha_s^3}{4} \frac{1}{A_\perp} \frac{dN^g}{dy} L \ln \frac{2E}{\mu^2 L} + \dots$. The outlined path length dependence holds for both small and large number of scatterings but $\frac{\omega dN^g}{d\omega}$ is more sensitive to the few semihard kicks that hard partons undergo as they traverse the medium [15]. Major corrections to the above analytic approximations arise from the finite kinematics which is particularly important at SPS and RHIC and even at the LHC for $p_T < 50$ GeV. These can be numerically evaluated as in [15].

For QGP in a local thermal equilibrium all dimensional scales can be related to the temperature: $\omega_{pl}^2 \sim \mu^2 \propto T^2$, $\rho_g \propto T^3$ and $\epsilon \propto T^4$. Moreover, gluon absorption [17] can significantly modify the radiative spectrum and the mean energy loss for small jet energies as shown in Figure 1a. The average energy gain from gluon absorption to first order in opacity, $\Delta E_{\text{abs}} = \frac{C_R \pi \alpha_s}{3} \frac{T^2}{\lambda_g E} L \ln \frac{\mu^2 L}{T} + \dots$, is power suppressed for large E but will manifest itself for $E < 5\mu$ via weaker hadron quenching. The reduction of available phase space for bremsstrahlung off heavy quarks, the dead cone effect [18], and the plasmon mass ω_{pl} Ter-Mikayelian effect have been systematically incorporated in the medium induced energy loss formalism [19] and shown to shorten the gluon formation times, $\tau_f^{-1} \rightarrow \tau_f^{-1} + \frac{\omega_{pl}^2 + \omega^2 M_q^2 / E^2}{2\omega}$, and regulate the color current propagators, $\frac{k_\perp^2}{k_\perp^2} \rightarrow \frac{k_\perp^2}{k_\perp^2 + \omega_{pl}^2 + \omega^2 M_q^2 / E^2}$. The dependence of $\frac{\Delta E}{E}$ on the heavy quark mass is illustrated in Figure 1a. In addition to a reduction of the mean energy loss the path length dependence of ΔE in static plasmas was found to be closer to the linear incoherent Bethe-Heitler regime [19, 20].

Approximate ways of estimating the observable jet quenching effect on final state hadrons include a suppression of the hard partonic cross section [21] or an effective

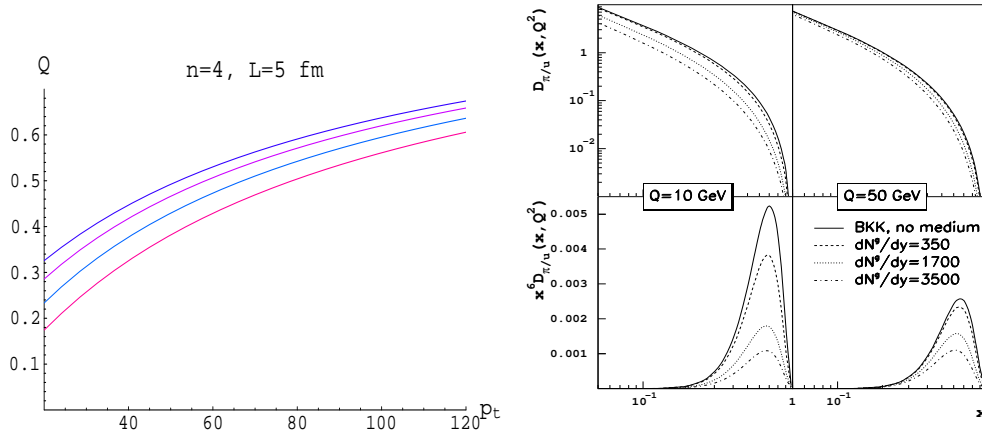


Figure 2. Left panel from [21]: typical asymptotic p_T dependence of the partonic quenching factor for LHC energies. Right panel from [22]: effective kinematic modification of the fragmentation functions versus $x = p_h/p_c$.

attenuation of the fragmentation functions [22], $D_{eff}(z) = \int d\epsilon P(\epsilon) \frac{1}{1-\epsilon} D\left(\frac{1}{1-\epsilon}\right)$. Here $P(\epsilon)$ is the probability of fractional energy loss $\epsilon = \sum_i \frac{\omega_i}{E}$ due to multiple gluon emission [21, 22]. These incorporate the same kinematic modifications to the leading hard parton which originate from the medium induced gluon bremsstrahlung at a timescale $t_0 = \frac{1}{Q} < t_{\text{radiation}} < t_{\text{hadronization}} = \frac{2z(1-z)E_{\text{parton}}}{\Lambda_{\text{QCD}}^2}$. The former approach is illustrated in Figure 2a for a static QGP with $\hat{q} = \frac{\mu^2}{\lambda_g} = 1 \frac{\text{GeV}^2}{\text{fm}}$ and the latter is exemplified in Figure 2b for $D_{u/\pi}(z, Q^2)$. Quantitative application, however, require the incorporation of energy loss calculations within the full perturbative QCD hadron production formalism [23].

2. Applications of jet tomography

Semi-inclusive deeply inelastic scattering (DIS) is an ideal probe of final state quark energy loss in cold nuclear matter. The known lepton E_l, E'_l and hadron E_h energies allow for an approximate reconstruction of the effective modification to the measured cross section $\sim D_{h/q}^{eA}(z)/D_{h/q}^{ep}(z)$, where $z = E_h/\nu$. Induced gluon bremsstrahlung was shown to result in an effective shift, $\Delta z \propto \alpha_s A^{2/3} \ln \frac{1}{x_B}$, of the fragmentation momentum fraction [24]. Comparison of HERMES data on the nuclear modification for ^{14}N and ^{84}Kr targets to theoretical calculations in Figure 3b provides strong evidence in support of the L^2 dependence of ΔE for static systems. The absorptive power of the medium for quark jets was found to be $-\frac{dE_q}{dz} = 0.5 \frac{\text{GeV}}{\text{fm}}$. Constraints on the cold nuclear matter transport coefficient can also be obtained from the analysis of Drell-Yan data on initial state broadening and energy loss [25]. The extracted $\frac{\mu^2}{\lambda_g} = 0.14 \pm 0.1 \frac{\text{GeV}^2}{\text{fm}}$ can be used to predict the final state hadronic suppression. Figure 3b shows the consistency of this approach on the example of the ν -dependent quenching.

The initial discovery of a qualitatively large high- p_T particle deficit at RHIC

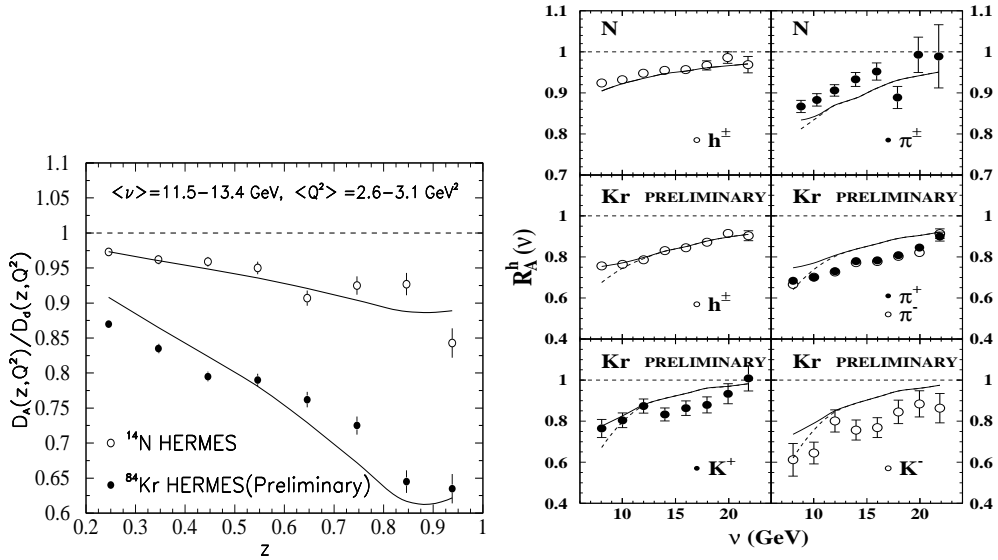


Figure 3. Left panel from [24]: evidence for the quadratic dependence of ΔE on the $L \propto A^{1/3}$ system size in semi-inclusive DIS. Hadron quenching is shown versus E_h/ν . Right panel from [25]: calculated $\nu = E - E'$ dependence of nuclear suppression with $\hat{q} = \frac{\mu^2}{\lambda g}$ fixed from Drell-Yan data.

$\sqrt{s}_{NN} = 130 \text{ GeV}$ [26] has revived the interest in hard physics in relativistic heavy ion reactions. However, it is the recent advances in the perturbative QCD description of multi-parton dynamics that have taken jet tomography to a new and quantitative level [12]. Figure 4a illustrates the predicted p_T dependence of R_{AA} versus \sqrt{s}_{NN} for central $Au + Au$ collisions [23]. The relative importance of the initial state multiple elastic scattering [10] relative to the final state radiative energy loss was found to decrease from SPS to the LHC. At high $Q^2 \sim p_T^2$ the $x < 0.1 - 0.01$ shadowing vanishes [27] but the small effects from the $x > 0.3$ EMC region are expected to persist. Figure 4b shows a good agreement of the calculated quenching for π^0 and h^\pm with $\frac{dN^g}{dy} = 1150$, comparable to the $y = 0$ net hadron rapidity density, with the precision high- p_T data at RHIC [5]. Ongoing re-analysis of the SPS data [28] is expected to establish a small hadronic suppression at $\sqrt{s}_{NN} = 17.4 \text{ GeV}$ and thus improve the agreement with the perturbative calculation in a medium of finite $\frac{dN^g}{dy} = 400 - 500$ soft parton density.

The centrality and rapidity dependence of jet quenching in $A + A$ reactions has also been addressed both analytically and numerically [29]. For 1+1D expansion hadronic attenuation scales with the number of participants as $R_{AA}(N_{\text{part}}) = [1 - (1 - (R_{AA}^{\text{central}})^{\frac{1}{n-2}})(N_{\text{part}})^{2/3}/(N_{\text{part}}^{\text{central}})^{2/3}]^{n-2}$ and is insensitive to the effective partonic slope n . As a function of rapidity $R_{AA}(y) \approx R_{AA}(y = 0)$ in agreement with the BRAHMS results [9]. Corrections to these estimates arise from the interplay of soft and hard physics and the steepening of particle spectra with rapidity $|y - y_{\text{mid}}|$.

Di-hadron tomography [30, 31, 32] is one of the new and promising direction of moderate- and high- p_T studies of in-medium jet modification. The differential cross section $\frac{d\sigma^{h_1 h_2}}{dy_1 dy_2 dp_{T1} dp_{T2} d\Delta\phi}$ is more sensitive to the non-Abelian dynamics when

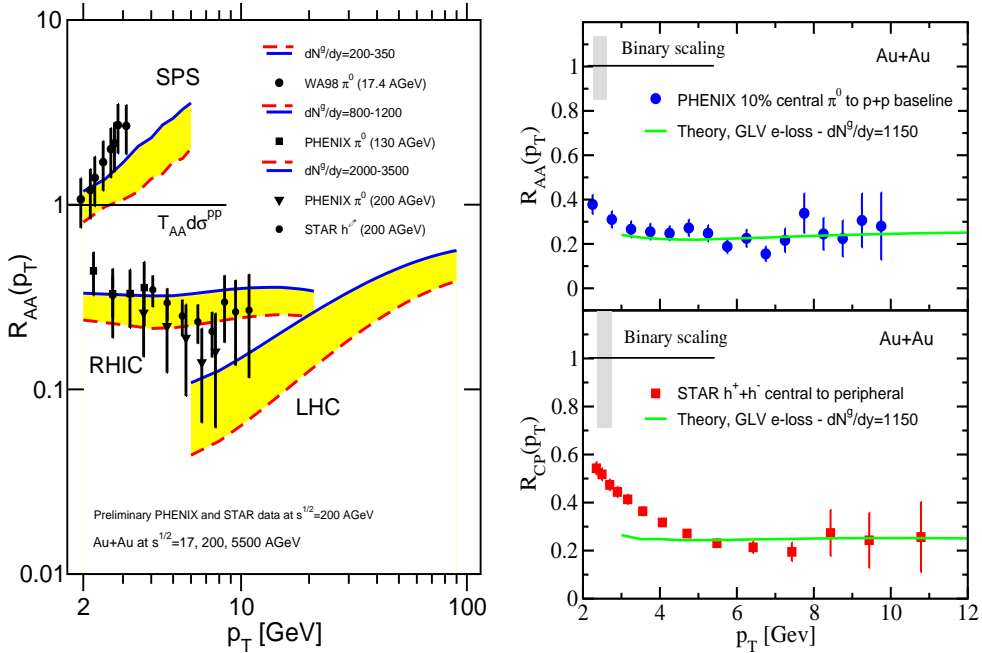


Figure 4. Left panel from [23]: predicted $\sqrt{s_{NN}}$ and p_T dependence of jet quenching for finite kinematics and finite system size. Right panel from [23]: comparison of the calculated approximately constant R_{AA} for π^0 and h^\pm to finalized experimental data.

compared to the single inclusive measurements. Triggering on a large transverse momentum particle biases the hard scatter toward the surface of the interaction region and the away-side partner carries most of the observable effect from the interactions in dense nuclear matter. On the example of the correlation function $C_2(\Delta\phi) = \frac{1}{N_{\text{trig}}} \frac{dN^{h_1 h_2}}{d\Delta\phi} \approx A_{\text{Near}} \exp\left(-\frac{\Delta\phi}{2\sigma_{\text{Near}}^2}\right) + A_{\text{Far}} \exp\left(-\frac{(\Delta\phi - \pi)}{2\sigma_{\text{Far}}^2}\right)$ energy loss reduces the area $\propto A_{\text{Far}}$ under the away-side peak. Figure 5a show a simulation of the disappearance of the back-to back correlations in a hydro+jet model [30] which is qualitatively consistent with the data. Important progress in di-jet correlation analysis has been made through recent studies of the attenuation effect relative to the reaction plane [32]. It confirms the $\Delta E \propto L$ path length dependence of energy loss in an expanding quark-gluon plasma [7]. Di-jet acoplanarity reflects the accumulated mean transverse momentum kick $\langle k_T^2 \rangle = \langle k_T^2 \rangle_{\text{vac}} + \langle k_T^2 \rangle_{\text{IS}} + \langle k_T^2 \rangle_{\text{FS}}$ of a hard scattered parton pair [31] and is measurable [32] via the enhanced away-side width σ_{Far} . Preliminary results for $d + Au$ and central $Au + Au$ collisions suggest a significant difference in the observed effect consistent with final state interactions in media of very different density and scattering power $\frac{\mu^2}{\lambda_g}$. A large σ_{Far} enhancement in central $Au + Au$ reactions may also indicate a power-law non-Gaussian semi-hard multiple scattering [33].

3. Future directions in jet quenching studies

Improved experimental techniques for jet cone reconstitution in the high-multiplicity environment of relativistic heavy ion reactions [32, 34] open new possibilities for

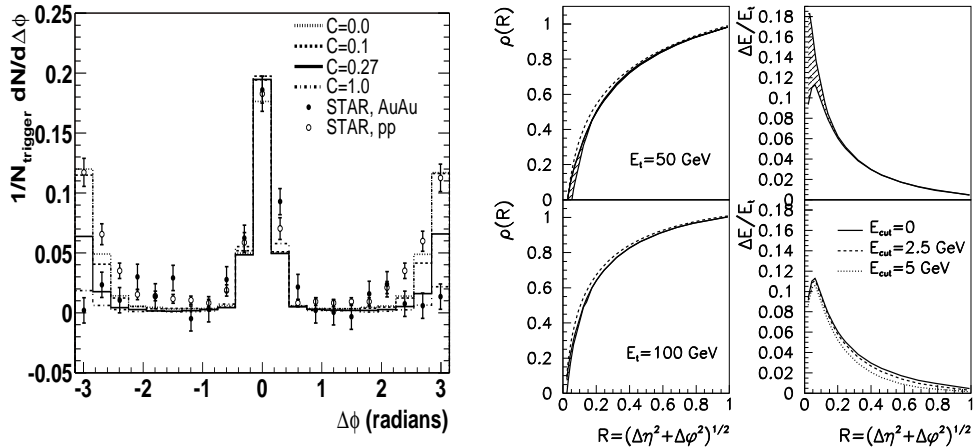


Figure 5. Left panel from [30]: disappearance of the away side correlation function in a hydro+jet model. Right panel from [35]: minimal $\sim 5\%$ modification to the intra-jet correlations for approximately collinear gluon bremsstrahlung.

differential studies of the jet properties. The transverse momentum broadening of the interacting parent parton+gluon system is expected to modify the intra-jet correlations and widen the jet cone [12, 35]. A quantitative measure of this effect will be the deposition of smaller fractional transverse energy $\rho(R) = \frac{1}{N_{\text{jets}}} \sum_{\text{jets}} \frac{\Delta E_T(R)}{\Delta E_T(R=1)}$ inside a cone of opening angle $R = \sqrt{\Delta\phi^2 + \Delta\eta^2}$ relative to the $p+p$ case. Simulations of this effect in Figure 5b at LHC bulk matter densities show that this effect is very small $\sim 5\%$ even for narrow cones $R = 0.3$ [35]. Perturbative calculations of di-hadron fragmentation also find insignificant alteration of the near-side correlation function [35].

While the approximate collinearity of the medium induced gluon bremsstrahlung suggests that modifications of the jet shape may be difficult to measure experimentally, a more promising way to verify the predictions of non-Abelian energy loss theory [12] may be to search for the “remnants of lost jets” [36]. The energy radiated off the leading parton is redistributed in the system, possibly within the jet cone itself. If it is subsequently fully thermalized, the increase in the soft gluon multiplicity can be estimated as $\Delta N^h \approx \frac{1}{4} \Delta S = \frac{1}{4} \frac{\Delta E}{T}$. Figure 6a shows the momentum density of hadrons $\rho(p_x)$ associated with back-to-back jets embedded in a parton cascade [36] and the reappearance of the lost energy at $p_x \approx p_T = 600$ MeV.

The long formation times τ_f , which are the basis of the non-Abelian LPM effect, may limit the possibility for secondary interactions of the radiative quanta. In this case one expects fewer harder gluons with $\omega > \omega_{\text{pl}}$ [15, 19, 22]. As a function of the experimental $p_{T\text{cut}}$ the accessible $N_{\text{parton}}(p_{T\text{cut}}) = 1|_{E-\Delta E \geq p_{T\text{cut}}} + P_0(\bar{N}_g)^{-1} \sum_n n P_n(\bar{N}_g)|_{\Delta E/n \geq p_{T\text{cut}}}$, with \bar{N}_g and the probability distribution $P_n(\bar{N}_g)$ computed numerically as in [22, 23]. Figure 6b shows that already at $p_T \simeq 1.5$ GeV a large fraction of the induced multiplicity is recovered and for $\lim_{p_{T\text{cut}} \rightarrow 0} E(p_T) = E_{\text{jet}}^{\text{tot}}$ and $\lim_{p_{T\text{cut}} \rightarrow 0} N_{\text{parton}}(p_{T\text{cut}}) = \bar{N}_g(E_{\text{jet}}) + 1$. I propose that upcoming comparison of the low- p_T experimental data on hadron multiplicities associated with energetic di-jets to theoretical calculations may provide an experimental handle on the degree of thermalization of the medium induced semi-hard bremsstrahlung.

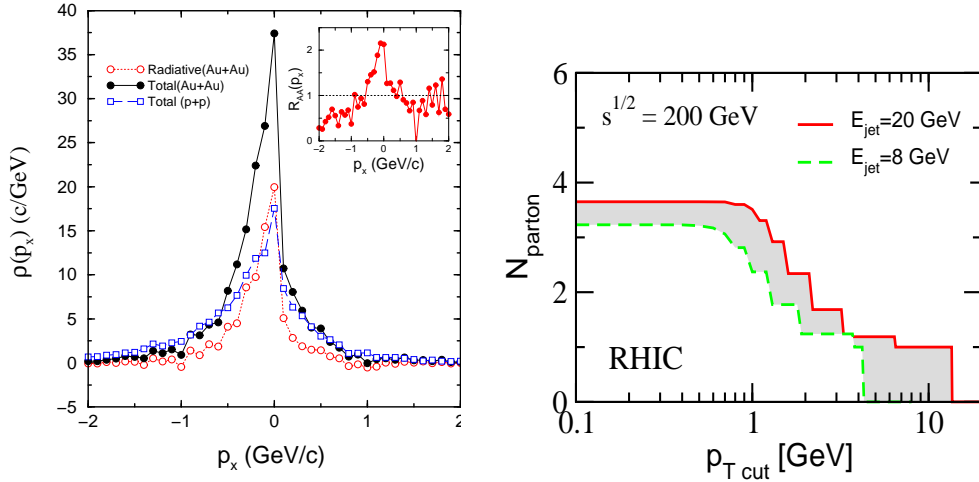


Figure 6. Left panel from [36]: momentum density of hadrons associated with energetic back-to-back jets with and without medium induced bremsstrahlung. Right panel from [36]: induced partonic multiplicity as a function of the experimental p_T cut for energetic quark jets.

4. Summary and conclusions

In this talk I emphasized the quantitative applications of the theory and phenomenology of medium-induced non-Abelian energy loss in reactions involving nuclei.

In QCD processes cold nuclear matter can be systematically characterized by its scattering and absorptive power. Table 1, adapted from [37], collects results from recent studies of semi-inclusive DIS hadron attenuation, Drell-Yan broadening and the Cronin enhancement. Within the uncertainties inherent in the theory of strong interactions different approaches consistently find $\frac{\mu^2}{\lambda_g} = 0.1 - 0.14 \frac{\text{GeV}^2}{\text{fm}}$ and final state $\langle -\frac{dE_q}{dz} \rangle = 0.4 - 0.6 \frac{\text{GeV}}{\text{fm}}$ for large nuclei.

In ultrarelativistic heavy ion reactions results of the jet tomographic analysis [23] based on the assumptions of local thermal equilibrium and longitudinal Bjorken expansion are presented in Table 2. For their interpretation we recall that lattice calculations with improved Wilson and staggered fermions suggest $T_c = 171 \pm 4$ MeV for 2-flavor QCD, $T_c = 154 \pm 6$ MeV for 3-flavor QCD and $\epsilon_c = (0.5 - 1) \frac{\text{GeV}}{\text{fm}^3}$ [38]. Although the energy density at SPS may have reached or even exceeded the critical value for a phase transition, the lifetime of the QGP $\tau_{tot} - \tau_0 \leq 1$ fm seems insufficient to clearly develop many of the signatures of deconfinement and collectivity. In contrast, at RHIC $T_0 = 380 - 400$ MeV $\geq 2T_c$, $\epsilon_0 = 14 - 20 \frac{\text{GeV}}{\text{fm}^3} \sim 100 \epsilon_{\text{cold}}$ and $\tau_{tot} - \tau_0 \sim 6$ fm is comparable to the transverse extent of the system itself. These initial conditions are in accord with the hydrodynamic estimates [39] based on the bulk properties of the plasma. Even a sizable theoretical error in the determination of $\frac{dN^g}{dy}$ is unlikely to qualitatively change RHIC's status on the QCD phase diagram. One should also note the much higher T_0 , ϵ_0 and the significantly longer lifetime of the QGP phase expected at the LHC.

In conclusion, jet tomographic analysis at RHIC presents strong evidence for the creation of the deconfined state of QCD. Future jet cone, di-jet correlation and energy

balance studies are expected to map out the properties of the plasma and reveal details of the QCD multiparton dynamics in ultradense nuclear matter.

Table 1. Summary of the transport and absorptive properties of cold nuclear matter of energy density $\epsilon_{\text{cold}} = m_N / (\frac{4}{3} \pi r_0^3) = 0.14 \frac{\text{GeV}}{\text{fm}^3}$ adapted from Ref. [37].

	$\frac{\mu^2}{\lambda_g} \left[\frac{\text{GeV}^2}{\text{fm}} \right]$	$\langle -\frac{dE_q}{dz} \rangle \left[\frac{\text{GeV}}{\text{fm}} \right]$
Semi-inclusive DIS quenching	0.12	0.5
Drell-Yan analysis	0.14 ± 0.1	0.6 ± 0.45
Cronin effect analysis	$0.10 - 0.14$	$0.4 - 0.6$
Theoretical estimates	0.05	0.2

Table 2. Summary of the properties of hot nuclear matter extracted via the jet tomographic analysis of Ref. [23]. To highlight the difference relative to the case of cold nuclear matter $\langle -\frac{dE_q}{dz} \rangle$ is estimated for a static plasma with the specified initial conditions.

	τ_0 [fm]	τ_{tot} [fm]	T_0 [MeV]	$\epsilon_0 \left[\frac{\text{GeV}}{\text{fm}^3} \right]$	$\frac{dN^g}{dy}$	$\langle -\frac{dE_q}{dz} \rangle \left[\frac{\text{GeV}}{\text{fm}} \right]$
SPS	0.8	1.4 – 2	210 – 240	1.5 – 2.5	200 – 350	2 – 3.5
RHIC	0.6	6 – 7	380 – 400	14 – 20	800 – 1200	7 – 10
LHC	0.2	18 – 23	710 – 850	190 – 400	2000 – 3500	17 – 28

Acknowledgments

Useful discussion with M. Gyulassy and J.W. Qiu is gratefully acknowledged. This work is supported by the United States Department of Energy under Grant No. DE-FG02-87ER40371.

References

- [1] I. Lovas, K. Sailer and Z. Trocsanyi, J. Phys. G **15**, 1709 (1989); M. Gyulassy, Lect. Notes Phys. **583**, 37 (2002).
- [2] K. J. Eskola and H. Honkanen, Nucl. Phys. A **713**, 167 (2003); I. Vitev, arXiv:hep-ph/0212109; B. Jager *et al.*, Phys. Rev. D **67**, 054005 (2003); D. de Florian, Phys. Rev. D **67**, 054004 (2003); P. Levai *et al.*, arXiv:nucl-th/0306019.
- [3] G. T. Bodwin, Phys. Rev. D **31**, 2616 (1985); J. C. Collins, D. E. Soper and G. Sterman, Nucl. Phys. B **261**, 104 (1985); Adv. Ser. Direct. High Energy Phys. **5** (1988) 1; J. W. Qiu and G. Sterman, Nucl. Phys. B **353**, 137 (1991); R. Brock *et al.*, Rev. Mod. Phys. **67**, 157 (1995).
- [4] X. N. Wang and M. Gyulassy, Phys. Rev. Lett. **68**, 1480 (1992); J. D. Bjorken, FERMILAB-PUB-82-059-THY.
- [5] S. S. Adler *et al.*, Phys. Rev. Lett. **91**, 072301 (2003); B. B. Back *et al.*, Phys. Lett. B **578**, 297 (2004); J. Adams *et al.*, Phys. Rev. Lett. **91**, 172302 (2003).
- [6] C. Adler *et al.*, Phys. Rev. Lett. **90**, 082302 (2003).
- [7] X. N. Wang, Phys. Rev. C **63**, 054902 (2001); M. Gyulassy, I. Vitev and X. N. Wang, Phys. Rev. Lett. **86**, 2537 (2001); M. Gyulassy *et al.*, Phys. Lett. B **526**, 301 (2002); D. Molnar and M. Gyulassy, Nucl. Phys. A **697**, 495 (2002); E. V. Shuryak, Phys. Rev. C **66**, 027902 (2002). I. P. Lohhtin *et al.*, Phys. Atom. Nucl. **65**, 943 (2002). A. Drees, H. Feng and J. Jia, arXiv:nucl-th/0310044.

- [8] I. Vitev and M. Gyulassy, Phys. Rev. C **65**, 041902 (2002); R. J. Fries *et al.*, Phys. Rev. Lett. **90**, 202303 (2003); V. Greco, C. M. Ko and P. Levai, Phys. Rev. Lett. **90**, 202302 (2003).
- [9] I. Arsene *et al.*, Phys. Rev. Lett. **91**, 072305 (2003); S. S. Adler *et al.*, Phys. Rev. Lett. **91**, 072303 (2003); B. B. Back, Phys. Rev. Lett. **91**, 072302 (2003); J. Adams *et al.*, Phys. Rev. Lett. **91**, 072304 (2003).
- [10] Y. Zhang, *et al.*, Phys. Rev. C **65**, 034903 (2002); I. Vitev, Phys. Lett. B **562**, 36 (2003); X. N. Wang, Phys. Lett. B **565**, 116 (2003); A. Accardi and M. Gyulassy, arXiv:nucl-th/0308029; X. F. Zhang and G. Fai, arXiv:hep-ph/0306227.
- [11] X. N. Wang, M. Gyulassy and M. Plumer, Phys. Rev. D **51**, 3436 (1995); M. Gyulassy and X. N. Wang, Nucl. Phys. B **420**, 583 (1994).
- [12] M. Gyulassy *et al.*, arXiv:nucl-th/0302077; A. Kovner and U. A. Wiedemann, arXiv:hep-ph/0304151; R. Baier, D. Schiff and B. G. Zakharov, Ann. Rev. Nucl. Part. Sci. **50**, 37 (2000).
- [13] B. G. Zakharov, JETP Lett. **63**, 952 (1996); JETP Lett. **64**, 781 (1996); U. A. Wiedemann, Nucl. Phys. B **582**, 409 (2000); Nucl. Phys. B **588**, 303 (2000).
- [14] R. Baier *et al.*, Nucl. Phys. B **483**, 291 (1997); Nucl. Phys. B **484**, 265 (1997). Nucl. Phys. B **531**, 403 (1998).
- [15] M. Gyulassy, P. Levai and I. Vitev, Nucl. Phys. B **594**, 371 (2001); Phys. Rev. Lett. **85**, 5535 (2000); Nucl. Phys. B **571**, 197 (2000).
- [16] B. W. Zhang and X. N. Wang, Nucl. Phys. A **720**, 429 (2003); J. Osborne and X. N. Wang, Nucl. Phys. A **710**, 281 (2002); X. N. Wang and X. F. Guo, Nucl. Phys. A **696**, 788 (2001).
- [17] E. Wang and X. N. Wang, Phys. Rev. Lett. **87**, 142301 (2001).
- [18] Y. L. Dokshitzer and D. E. Kharzeev, Phys. Lett. B **519**, 199 (2001).
- [19] M. Djordjevic and M. Gyulassy, arXiv:nucl-th/0310076; Phys. Rev. C **68**, 034914 (2003); Phys. Lett. B **560**, 37 (2003).
- [20] B. W. Zhang, E. Wang and X. N. Wang, arXiv:nucl-th/0309040; N. Armesto, C. A. Salgado and U. A. Wiedemann, arXiv:hep-ph/0312106.
- [21] R. Baier, Y. L. Dokshitzer, A. H. Mueller and D. Schiff, JHEP **0109**, 033 (2001).
- [22] M. Gyulassy, P. Levai and I. Vitev, Phys. Lett. B **538**, 282 (2002); C. A. Salgado and U. A. Wiedemann, Phys. Rev. Lett. **89**, 092303 (2002).
- [23] I. Vitev and M. Gyulassy, Phys. Rev. Lett. **89**, 252301 (2002); I. Vitev, arXiv:nucl-th/0308028.
- [24] E. Wang and X. N. Wang, Phys. Rev. Lett. **89**, 162301 (2002).
- [25] F. Arleo, Eur. Phys. J. C **30**, 213 (2003); JHEP **0211**, 044 (2002); Phys. Lett. B **532**, 231 (2002).
- [26] K. Adcox *et al.*, Phys. Rev. Lett. **88**, 022301 (2002); P. Levai *et al.*, Nucl. Phys. A **698**, 631 (2002).
- [27] J. W. Qiu and I. Vitev, arXiv:hep-ph/0401062; arXiv:hep-ph/0309094; K. J. Eskola, V. J. Kolhinen and C. A. Salgado, Eur. Phys. J. C **9**, 61 (1999); H. J. Pirner and J. P. Vary, Phys. Rev. Lett. **46**, 1376 (1981).
- [28] D. d'Enterria, these proceedings; D. d'Enterria, in preparation.
- [29] G. G. Barnafoldi *et al.*, arXiv:hep-ph/0311343; G. G. Barnafoldi, arXiv:hep-ph/0312384; A. Adil, M. Gyulassy and I. Vitev, in preparation; A. Polleri and F. Yuan, arXiv:nucl-th/0108056; T. Hirano and Y. Nara, Phys. Rev. C **68**, 064902 (2003).
- [30] T. Hirano and Y. Nara, Phys. Rev. Lett. **91**, 082301 (2003); T. Hirano and Y. Nara, Phys. Rev. C **66**, 041901 (2002);
- [31] J. W. Qiu and I. Vitev, Phys. Lett. B **570**, 161 (2003); X. N. Wang, arXiv:nucl-th/0305010.
- [32] J. Rak arXiv:nucl-ex/0306031; these proceedings; J. Bielcikova *et al.*, Phys. Rev. C **69**, 021901 (2004); M. Miller, these proceedings; K. Filimonov, these proceedings.
- [33] M. Gyulassy, P. Levai and I. Vitev, Phys. Rev. D **66**, 014005 (2002).
- [34] F. Wang, these proceedings.
- [35] C. A. Salgado and U. A. Wiedemann, arXiv:hep-ph/0310079; A. Majumder and X. N. Wang, arXiv:hep-ph/0402245.
- [36] S. Pal and S. Pratt, Phys. Lett. B **574**, 21 (2003); I. Vitev, energy loss simulation based on the Reaction Operator approach.
- [37] F. Arleo, contribution to the CERN Yellow Report on Hard Probes in Heavy Ion Collisions at the LHC; A. Accardi *et al.*, arXiv:hep-ph/0310274.
- [38] F. Karsch, Nucl. Phys. A **698**, 199 (2002); Lect. Notes Phys. **583**, 209 (2002); F. Karsch, E. Laermann and A. Peikert, Phys. Lett. B **478**, 447 (2000).
- [39] P. F. Kolb and U. Heinz, arXiv:nucl-th/0305084; arXiv:nucl-th/0305064; T. Hirano, these proceedings; Y. Nara, these proceedings.